Copyright © [2012] IEEE. Reprinted from IEEE WHISPERS June 2012.

This material is posted here with permission of the IEEE. Internal or personal use of this material is permitted. However, permission to reprint/republish this material for advertising or promotional purposes or for creating new collective works for resale or redistribution must be obtained from the IEEE by writing to pubs-permissions@ieee.org. By choosing to view this document, you agree to all provisions of the copyright laws protecting it.

See next page.

QUICK ATMOSPHERIC CORRECTION (QUAC) CODE FOR VNIR-SWIR SPECTRAL IMAGERY: ALGORITHM DETAILS

Lawrence S. Bernstein, Steven M. Adler-Golden, Xuemin Jin, Brian Gregor and Robert L. Sundberg

Spectral Sciences, Inc., Burlington MA 01803-3304

ABSTRACT

We describe an in-scene method for VNIR-SWIR atmospheric correction for multi- and hyperspectral imagery, dubbed QUAC (QUick Atmospheric Correction). It determines the atmospheric compensation parameters directly from the information contained within the scene using the observed pixel spectra. The approach is based on the empirical finding that the mean spectrum of a collection of diverse material spectra, such as the endmember spectra in a scene, is essentially invariant from scene to scene. It allows the retrieval of reasonably accurate reflectance spectra even when the sensor does not have a proper radiometric or wavelength calibration, or when the solar illumination intensity is unknown. The computational speed of the atmospheric correction method is significantly faster than for the first-principles methods, making it potentially suitable for real-time applications. QUAC is applied to atmospheric correction of example AVIRIS and HyMap data sets. Comparisons to the physics-based FLAASH code are also presented.

Index Terms— atmospheric correction, hyperspectral

1. INTRODUCTION

When gazing out the window of an aircraft, the solar-illuminated surface features are often difficult to discern because the intervening atmosphere has degraded the image quality. This degradation results from both atmospheric attenuation of the surface reflected light as well as loss of contrast due to an intervening white haze from sunlight scattering by atmospheric aerosols and molecules. For remotely sensed imagery, typically taken from aircraft and satellite-based sensors, it is routinely required that these atmospheric effects be removed from the imagery, in order to retrieve the inherent spectral reflectance of the surface materials. This enables the surface materials to be identified through comparison to a library of well-characterized material spectra. The process for removing the atmospheric effects is referred to as atmospheric correction (or compensation). An example of the application of atmospheric correction to hyperspectral imagery is shown in Figure 1.

Many atmospheric correction methods and algorithms exist, including those based on first-principles radiation transport (RT) calculations[1-8] and empirical approaches such as the Empirical Line Method (ELM) [9], which relies on two or more known reflectances in the image. However, none of these methods provide the ideal combination of high accuracy, high computational speed, and independence from prior knowledge (i.e., ground truth, sensor calibration, measurement geometry, etc.). In 2004 we introduced a new atmospheric correction algorithm and code called QUAC® (QUick Atmospheric Correction) [10-11] which comes close to satisfying these attributes.

®QUAC is a registered trademark of Spectral Sciences, Inc.

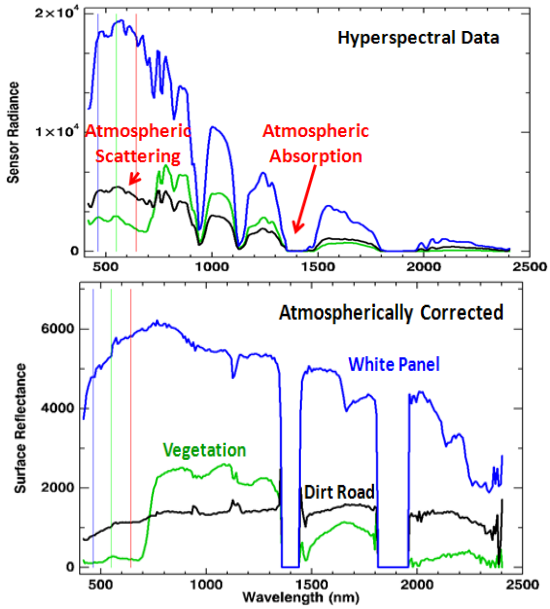

Fig 1. An example of atmospheric correction processing for hyperspectral imaging sensors, showing several at-sensor pixel spectra (top) and their corresponding atmospherically corrected surface reflectance spectra (bottom). Because atmospheric attenuation in the 1400 and 1900 nm regions is strong, it is not possible to correct these regions.

QUAC is an in-scene approach, requiring only approximate specification of sensor band locations (i.e., central wavelengths) and their radiometric calibration; no additional metadata is required. Because QUAC does not involve first principles RT calculations, it is much faster than the physics-based methods; however, it is also more approximate. Previous comparisons to the most widely used physics-based code, FLAASH (Fast Line-of-sight Atmospheric Analysis of Spectral Hypercubes), have shown that the absolute accuracy of QUAC is ~±15% with respect to FLAASH-retrieved reflectances for well-calibrated data and well-characterized measurement conditions [11]. A comparison of QUAC and FLAASH is presented in Figure 2, which exhibits the general trend that spectral shapes agree well and the largest differences are in the absolute normalization of the QUAC results. While the accuracy of the physics-based methods is directly tied to the accuracy of the sensor calibration and measurement geometry, QUAC performance will not significantly degrade as sensor and measurement uncertainties increase. Finally, in contrast to the physics-based methods, which require the presence of specific bands in order to correct for water absorption and aerosol scattering, QUAC works with any collection of VNIR-SWIR (e.g., VNIR only or SWIR only) bands for both multispectral and hyperspectral sensors.

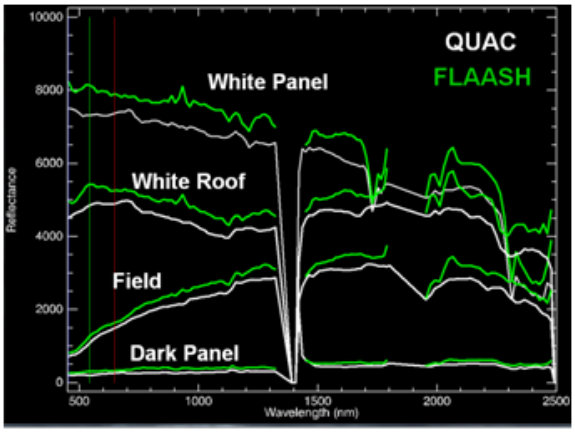

Fig 2. Comparison of QUAC and FLAASH results for a well ground-truthed HyMap data collect over Davis, CA.

2. ALGORITHM DESCRIPTION

The basic physics behind atmospheric correction is depicted in Figure 3. The observed spectral radiance, L_{obs}, for a pixel with surface reflectance, ρ_{sur}, is the sum of the three paths in Figure 3,

$$L_{obs} = (A + C\rho_{ave}) + B\rho_{sur}. \quad \textbf{(1)}$$

The components in ($A+C\rho_{ave}$) are grouped together because they are approximately constant over an image, and thus, can be considered as an Offset common to all the image pixels. This simple linear relationship can be re-arranged to express the retrieved surface reflectance in terms of the observed signal and derived atmospheric parameters,

$$\rho_{sur} = Gain(L_{obs} - Offset), \quad \textbf{(2)}$$

where the Gain=1/B, and the Offset=($A+C\rho_{ave}$). For a physics-based approach, A, B, and C are retrieved by comparison of certain spectral features to those predicted by RT calculations. For QUAC, we determine these parameters directly from the in scene spectral data and a key underlying assumption.

For QUAC, the Gain and Offset are given by,

$$Gain = \frac{<\rho_{end}>_{lib}}{<(L_{obs} - C\rho_{ave})_{end}>}, \text{ and} \quad \textbf{(3)}$$

$$Offset = darkest\ pixel\ value\ for\ each\ band \quad \textbf{(4)}$$

where $<\rho_{end}>_{lib}$ is the average of the endmember spectra representing a reference library of material reflectance spectra, and $<(L_{obs}\text{-}C\rho_{ave})_{end}>$ is the average of a collection of endmembers retrieved from the observed, in-scene pixel spectra. An endmember represents a unique spectrum from a collection of spectra. In most cases, linear combinations of a small number of endmember spectra (i.e., ~10-100) can accurately represent a large number of spectra associated with a spectral library or image (i.e., >10,000). In QUAC, we use the SSI-developed SMACC (Sequential Maximum Angle Convex Cone) code to find endmembers [12].

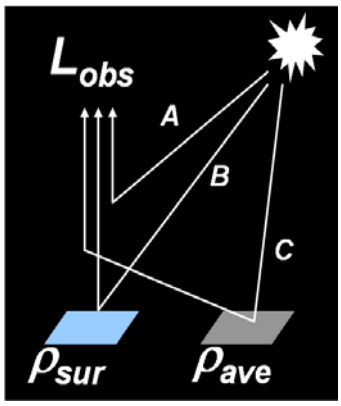

Fig 3. The three types of paths, A, B, and C, that solar photons can travel on their way to a remotely located observer, where ρ_{sur} is the reflectance of the observed surface pixel, ρ_{ave} denotes the average reflectance of the surrounding pixels, and L_{obs} is the sensor radiance corresponding to the observed surface pixel.

The key QUAC assumption, which empirically holds for most scenes, is that the average of the endmember reflectance spectra, which are not highly structured (i.e., excluding vegetation, mud, etc.), is always the same. More specifically, every image is assumed to contain at least a handful (~10 or more) of spectrally diverse materials whose average reflectance spectrum can be taken as a "universal" reference. The materials may include both natural and manmade materials, such a dirt field, a water body, rocks, cars, roofs, roads, etc. It is unusual that this material diversity condition is not met, but it can occur, for example, in some all-water or all-desert scenes, etc. However, such imagery is of little interest for most applications.

2.1 Determination of the reference reflectance spectrum

The "universal" reference spectrum is derived by finding and averaging endmember spectra from a diverse collection of natural and manmade library reflectance spectra. We compiled a reference library from the spectral libraries provided with ENVI [13]. Since the endmember representation of this library weeds out nearly degenerate spectra, it wasn't necessary to put a great deal of effort into selecting the library entries.

Typically, 50 scene endmembers are used in the correction process, and the reference spectrum is also based on the same number of endmembers. The average of these spectra provides the reference correction spectrum as displayed in Figure 4. For each run, QUAC uses both the same number of endmembers and also the same selection of sensor-specific spectral channels for determining the image and reference library endmembers.

The general shape of the reference reflectance spectrum has a simple physical origin. The decrease towards the long wavelength edge arises because the molecular constituents of materials have relatively strong near infrared vibrational absorption features that increase in strength with increasing wavelength. The decrease towards the short wavelength edge arises because the molecular constituents have strong electronic absorption features that increase in strength with decreasing wavelength. While, for reasons discussed later, we normalize the peak of this curve to unity, it is important to note that the peak average reflectance is ~0.4.

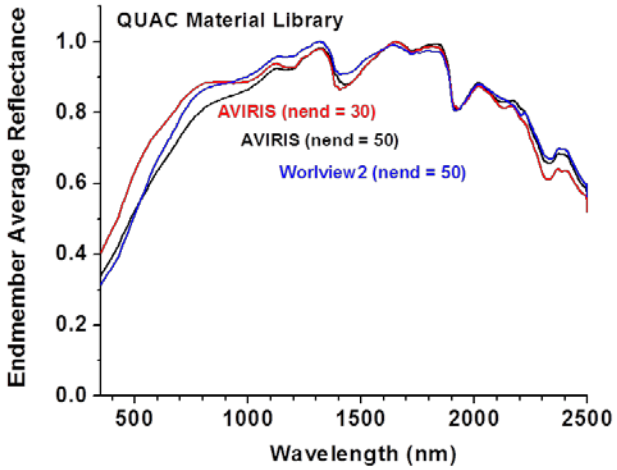

Fig 4. Averages of the library endmembers selected based on different sensors and different number of endmembers. The peak value of each curve has been normalized to 1.0.

Why does QUAC work, or equivalently, why should there be a "universal" reference spectrum? There is no first-principles reason for this, only a qualitative explanation of why an *approximately* "universal" curve is plausible. As can be seen by inspection of Figure 4, a collection of a large number of different material reflectance spectra non-uniformly span the ~0-0.8 range of reflectance values. We can expect most scenes to exhibit the same general behavior, that is, to contain a diversity of materials that approximately spans the 0-0.8 reflectance range. Near spectral duplicates and differences in abundances don't matter, since these issues are negated by finding the endmbember representation of the image pixels.

There are additional issues for real scenes and real sensor data, which need to be treated in the endmember selection process. For example, real scenes can exhibit solar glints, whose reflectances can far exceed 0.8. These excessively bright pixels need to be filtered out prior to endmember selection. Real sensors can have “bad” pixels with unphysical, highly structured spectra that can introduce spurious features into the Gain curve. The methods used in QUAC to filter out these and other types of spurious spectra are touched on below.

The Offset calculation involves a number of data conditioning steps to insure that a valid baseline is determined. This includes: (1) removal of border pixels, (2) averaging of adjacent pixels in a line, (3) rejecting values less than or equal to 0, and (4) median filtering of adjacent pixels to remove spike artifacts.

Prior to endmember selection the data is converted to an approximate 0-1 reflectance scale by dividing by the maximum value and an approximate solar blackbody curve normalized to unity at its peak value. It is not necessary, nor is it desirable, to use the exact solar blackbody curve. We adjust the effective solar temperature to yield approximate reflectance curves that span about the same range of values throughout the spectral domain of the sensor. The effective solar temperature varies between 4000 and 4500K, depending on the sensor type, as contrasted to the actual solar temperature of 5700K. There are two important reasons for transforming to a reflectance scale: (1) it simplifies the process of setting spectrally dependent filter thresholds, since all sensors are put on a common scale, and (2) it insures that all spectral regions are comparably weighted in the endmember selection process. The latter is particularly important because it maintains consistency with the selection of library endmembers, which is based on reflectance values.

It is important to filter out spectra that can introduce undesirable features and biases into the Gain curve. The most common example is vegetation, which has a strongly rising red edge around 700 nm (see Figure 1). Vegetation is often present and exhibits a lot of spectral variability, which means that many vegetation spectra would be selected as endmembers. This would produce a strong edge feature in the Gain curve around 700 nm and would result in a strong imbalance in the Gain to either side of the red edge. In QUAC we threshold pixels using the NDVI (Normalized Difference Vegetation Index) metric to discard pixels vegetation pixels. Before the final scene endmembers are determined, we filter out excessively bright pixels due to either glints or channel saturation.

As mentioned above, we need to set the absolute normalization for the Gain curve. We define two potential normalization values, based on different assumptions, and then select the preferred value. One method is defined by the absolute scale for the reference spectrum (i.e., before the peak value is normalized to unity). The other is based on an assumed typical peak value for the average strong vegetation spectrum, ~0.4 at 850 nm. Empirically, we have found that the preferred method is the one that yields the smaller reflectances value for the specific data cube.

3. EXAMPLE APPLICATION

Spectral additional comparisons between QUAC and FLAASH are shown in Figure 5 for an AVIRIS and Landsat-7 image. Both of the scenes presented here have a large variety of manmade and natural materials. The derived reflectance spectra are shown for vegetation, soil, water and reflective materials.

4. SUMMARY AND FUTURE WORK

QUAC is a semi-empirical algorithm for atmospheric correction for VNIR-SWIR spectral imaging sensors. Applications of QUAC to a wide assortment of spectral imaging data, such as HSI AVIRIS and HyMap data as well as MSI Landsat-7 data shows surprisingly good performance, nearly comparable to that of a first-principles physics-based code. Continued development and validation of QUAC is planned using a wider variety of HSI and MSI data sets. Computational speed-ups, automation and, eventually, the development of an on-board data processing capability will also be explored.

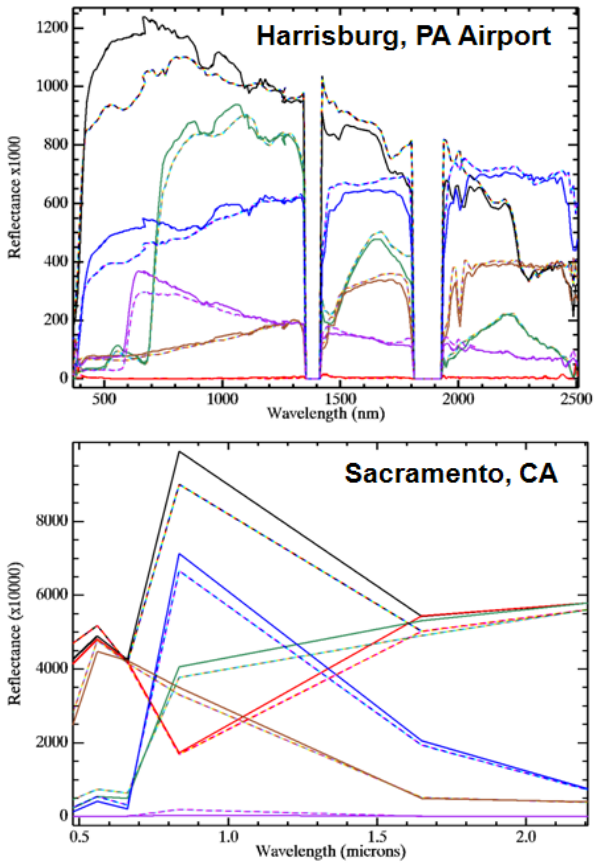

Fig 5. Comparisons of QUAC (dashed lines) and FLAASH (solid lines) reflectance spectra for the HSI AVIRIS (top) and MSI Landsat7 (bottom) data sets.

5. ACKNOWLEDGEMENTS

We appreciate the technical and administrative contributions of many individuals, including T. Perkins, M. Matthew, and M. Fox of Spectral Sciences, Inc., P. Villeneuve, A. Stocker, and R. O'Connor of Space Computer Corp., S. Allen of The Analytical Sciences Corp., J. Magarick, T. Smith, J. Nettles, G. Boer, and A. Sanders of the National Geospatial-Intelligence Agency, B. Thompson, M. Peitersen, and A. Ifarraguerri of Science Applications International Corp. We would also like to acknowledge financial support from Spectral Sciences, Inc.

6. REFERENCES

[1] Gao, B.-C., K.B. Heidebrecht, and A.F.H. Goetz, "Derivation of Scaled Reflectances from AVIRIS Data," *Proceedings of the Fourth Annual JPL Airborne Geoscience Workshop*, Vol. I. pp.35-36, 1993.

[2] Montes, M.J., B.-C. Gao, and C.O. Davis, "A new algorithm for atmospheric correction of hyperspectral remote sensing data," *SPIE Proceedings, Geo-Spatial Image and Data Exploitation II, Vol. 4383*, pp. 23-30, 2001.

[3] Green, R.O., D.A. Roberts, and J.E. Conel, "Characterization and Compensation of the Atmosphere for Inversion of AVIRIS Calibrated Radiance to Apparent Surface Reflectance," *Summaries of the Sixth Annual JPL Earth Science Workshop*, JPL Publication 96-4, Vol. 1, pp. 135-146, 1996.

[4] Miller, C. J., "Performance assessment of ACORN atmospheric correction algorithm," *SPIE Proceedings, Algorithms and Technologies for Multispectral, Hyperspectral, and Ultraspectral Imagery VIII*, 4725, pp. 438-449, 2002.

[5] Adler-Golden, S.M., M.W. Matthew, L.S. Bernstein, R.Y. Levine, A. Berk, S.C. Richtsmeier, P.K. Acharya, Anderson, G.P., G. Felde, J. Gardner, M. Hoke, L.S. Jeong, B. Pukall, J. Mello, A. Ratkowski and H.-H. Burke, "Atmospheric Correction for Short-wave Spectral Imagery Based on MODTRAN4," *Summaries of the Eighth Annual JPL Earth Science Workshop*, JPL Publication 99-17, pp. 12-23, Jet Propulsion Laboratory, Pasadena, CA., 1999.

[6] Matthew, M.W., S.M. Adler-Golden, A. Berk, G. Felde, G.P. Anderson, D. Gorodetzky, S. Paswaters and M. Shippert, "Atmospheric Correction of Spectral Imagery: Evaluation of the FLAASH Algorithm with AVIRIS Data," *SPIE Proceeding, Algorithms and Technologies for Multispectral, Hyperspectral, and Ultraspectral Imagery IX*, 5093, pp. 474-482, 2003.

[7] Qu, Z., A.F.H. Goetz, and B. Kindel, "High-accuracy Atmospheric Correction for Hyperspectral Data (HATCH)," *Proceedings of the Ninth AVIRIS Earth Sciences and Applications Workshop*, JPL Publication 00-18, pp. 373-380, Jet Propulsion Laboratory, Pasadena, CA, 2000.

[8] Richter, R. and D. Schlaepfer, "Geo-atmospheric processing of airborne imaging spectrometry data Part 2: atmospheric/topographic correction" *Int. J. Remote Sensing*, 23, 2631-2649, 2002.

[9] Roberts, D. A., Y. Yamaguchi, and R. J. P. Lyon, "Calibration of Airborne Imaging Spectrometer data to percent reflectance using field spectral measurements," *19th International Symposium on Remote Sensing of Environment*, Ann Arbor, MI, 1985.

[10] Bernstein, L. S., S. M. Adler-Golden, R. L. Sundberg, R. Y. Levine, T. C. Perkins, A. Berk, A. J. Ratkowski, and M. L. Hoke, "A New Method for Atmospheric Correction and Aerosol Optical Property Retrieval for Vis-SWIR Multi- and Hyperspectral Imaging Sensors: QUAC (QUick Atmospheric Correction)," *Proc. 13th JPL Airborne Earth Science Workshop*, April 2004.

[11] Bernstein, L. S., S. M. Adler-Golden, R. L. Sundberg, and A. J. Ratkowski, "In-scene-based atmospheric correction of uncalibrated VISible-SWIR (VIS-SWIR) hyper- and multispectral imagery," *Proc. SPIE Int. Soc. Opt. Eng.*, 7107, 2008.

[12] Gruninger, J., Lee, J. and Sundberg, R.L., "The Application of Convex Cone Analysis to Hyperspectral and Multispectral Scenes," *SPIE Proceedings Image and Signal Processing for Remote Sensing VIII*, Vol. 4888, pp. 188-198, (March 2003).

[13] Johns Hopkins University spectral library, available from http://speclib.jpl.nasa.gov/ (2006).